Materials Science & Engineering C 100 (2019) 631–644

Contents lists available at ScienceDirect

Materials Science & Engineering C

journal homepage: www.elsevier.com/locate/msec

Review

Advances in additive manufacturing for bone tissue engineering scaffolds

Ana Paula Moreno Madrid[a,b,c,*], Sonia Mariel Vrech[a,b], María Alejandra Sanchez[c], Andrea Paola Rodriguez[a,c]

[a] CONICET, National Scientific and Technical Research Council, Argentina
[b] CEMNCI, Faculty of Exact Sciences and Engineering, National University of Tucuman, Argentina
[c] LAMEIN, Faculty of Exact Sciences and Engineering, National University of Tucuman, Argentina

ARTICLE INFO

Keywords:
Scaffold
Bone
Tissue engineering
Additive manufacturing

ABSTRACT

This article reviews the current state of the art of additive manufacturing techniques for the production of bone tissue engineering (BTE) scaffolds. The most well-known of these techniques include: stereolithography, selective laser sintering, fused deposition modelling and three-dimensional printing. This review analyses in detail the basic physical principles and main applications of these techniques and presents a list of biomaterials for BTE applications, including commercial trademarks. It also describes and compares the main advantages and disadvantages and explains the highlights of each additive manufacturing technique and their evolution. Finally, is discusses both their capabilities and limitations and proposes potential strategies to improve this field.

1. Introduction

Bone tissue is known for its self-healing abilities. It undergoes dynamic remodelling, maturation, differentiation and controlled resorption. All these processes are achieved through a dynamic process involving osteoclasts and osteoblasts, which are responsible for maintaining a healthy bone [1]. However, large-scale bone defects cannot be healed completely by the body [2]. Schimitz and Hollinger [3] defined the critical size defect as the smallest intraosseous wound that would not heal by bone formation. In these cases, external treatment to restore normal functions is needed. The different treatment options include autografts (bone taken from the same person's body) and allografts (from a deceased donor). However, since more effective strategies to heal large bone defects are needed, are currently investigating new biomaterials and new scaffolding techniques. In this context, Bone Tissue Engineering (BTE) is a critical area of research.

Tissue Engineering (TE) typically involves the use of scaffolds, which provide structural support for the newly formed tissue. Scaffolds serve as temporary templates for the interactive traffic of cells as well as for the formation of the extracellular matrix [4]. The exploration of novel ideas in the design of these scaffolds, as well as of other complex biomedical models such as, prostheses and implants can be achieved by the application of computational modelling using patient-specific anatomical data, and can then be materialized by Additive Manufacturing (AM) techniques. Computational modelling allows selecting the suitable porosity, size and geometric design of each specific defect.

Scaffolds can be produced with different kinds of polymers and polymer-based composite materials, and several approaches can be applied to improve their biological and mechanical features. Maietta et al. [5], for example, have recently shown that Youngs modulus, a mechanical property that measures the stiffness of a solid material, can be improved by loading a polymer with organic and inorganic fillers. Also, Patricio et al. in 2018 [6] showed that the addition of two different polymers can improves the biomechanical properties of the constructs.

It should also be noted that the manipulation of the main features of the materials at the micro- and nano-metric scale offers a novel strategy to improve the biological and mechanical properties of scaffolds. This feature has been critically reviewed by Guarino et al. in 2012 [7].

The aim of this article is to review the information on AM techniques as a guide for anyone who needs to apply them for the production of BTE scaffolds. Section 2 explains the general concepts of TE and the specific requirements for BTE. Section 3 describes in detail the basic physical principles, main properties and applications as well as the evolution process of the following AM techniques: stereolithography, selective laser sintering, fused deposition modelling and three-dimensional printing. Table 1 summarises and compares the advantages and disadvantages of the above mentioned techniques. Finally, Section 4 presents discussions and recommendations on these techniques in terms of their applicable conditions for BTE.

* Corresponding author at: CONICET, National Scientific and Technical Research Council, Argentina.
E-mail addresses: paulamorenomadrid@gmail.com (A.P. Moreno Madrid), svrech@herrera.unt.edu.ar (S.M. Vrech).

https://doi.org/10.1016/j.msec.2019.03.037
Received 15 March 2018; Received in revised form 7 March 2019; Accepted 10 March 2019
Available online 13 March 2019
0928-4931/

Table 1
Scaffolds AM methods: a brief description and comparison.

Technique		Description	Main parameters	Advantages	Disadvantages	Ref.
SLA	Accuracy + + + Cost $$	This technology generates three-dimensional scaffolds by creating a cross-sectional pattern of the desired body in a fluid medium that solidifies in response to laser stimulation. Successive adjacent laminae, representing adjacent cross-sections of the object, are formed and integrated together providing a step-wise laminar build-up of it.	Layer thickness: 1 μm for specimen volumes smaller than 35 mm^3. Smallest feature: Indirect method: 366 μm. Direct method: 1–5 μm, 10–70 μm.	Complex internal features can be obtained. Growth factors, proteins and cell patterning are possible. Possibility of encapsulating cells.	Moderate strength. Photopolymer is needed. Support structure is needed. Single material. Post-curing is generally required. Few suitable biocompatible and biodegradable materials can be used. Distortion and shrinkage can occur.	[18,19,23–27]
SLS	Accuracy + + Cost $$$	This technique uses a laser emitting infrared radiation to selectively heat powder material just beyond its melting point. The laser traces the shape of each cross-section of the model to be built, sintering the powder in a thin layer. After each layer solidifies, the piston at the top of the model retracts to a new position and a new layer of powder is supplied using a mechanical roller.	Layer thickness: 76–100 μm. Smallest feature: 45–100 μm.	No support structure is needed. No post-processing is required.	High processing temperature. Powder can be trapped inside the body. Laser intensity can induce polymer degradation. Poor control over surface topography. Limited variety and high cost materials. Impossibility to include cells.	[18,20,24,27]
FDM	Accuracy + Cost $	Process involving a movable dispensing head provided with a supply of material which solidifies at a predetermined temperature, and a base member, which is moved along three perpendicular axis in a predetermined pattern to create three-dimensional objects by building-up material discharged from the dispensing head onto the base member at a controlled rate.	Layer thickness: 250–370 μm. Smallest feature: rod diameter: 260–700 μm.	Simple process. No platform or support needed (except for structure overhangs). High mechanical strengths. High production rate. Low cost. No materials trapped into the scaffold.	Limited variety of materials. Need of molten phase. Only extrudes filaments. Possible thermal degradation of polymers.	[18,21,25,26,28]
3DP	Accuracy + + Cost $$	This practice is based on the controlled deposition of a binder material laid on a powder layer. When the binder gets on to the powder, is solidifies layer by layer according to a CAD model. Finally, in many cases, it is subjected to a heat process to complete the bonding of the powder particles.	Layer thickness: Slurry method: 20–100 μm. Dry powder method: 50 μm. Smallest feature: from 350 to 500 μm	No material heating involved. No support material needed. High production rate. Wide range of material available.	Low green strength. Post-processing is needed. Post-processing procedure restricts biomolecule incorporation. Powder can be trapped inside the body.	[18,22,26]

2. Tissue engineering (TE): general concepts

TE is a developing field with a great potential in regenerative medicine. Landers et al. [8] defines TE as the application of principles and methods of engineering and life sciences towards the fundamental understanding of the complex structure-function of tissues and the development of biological substitutes to restore, maintain or improve tissue functions.

This field currently offers innovative strategies to implement biological substitutes in different medical fields. Major scientific advances in biomaterials, stem cells, growth and differentiation factors and tissue micro-environment have fallowed 'making' tissue in the laboratory by combining extracellular matrices, cells and biologically active molecules. Cells are seeded in artificial structures called scaffolds, which are able to behave as templates for tissue formation. These scaffolds are critical and the success of tissue regeneration depends on both, their macro- and micro-structure, as well as on the constituent biomaterials. Scaffolds must be able to reproduce the existing *in vivo* environment and to allow cells to exert influence. Tissue regeneration will depend on complex cell-cell and cell-scaffold interactions regarding the action of soluble factors, both locally and systemically. Seed cells may derive from different sources, including established cell lines, stem cells or primary cells (autologous, allogeneic or xenogeneic).

Ideally, the biomaterials selected to obtain scaffolds should allow one or more of the following functions:

- cell adhesion and migration,
- diffusion of vital cell nutrients and secreted products,
- vascularization,
- support of mechanical and biological functions in particular situations.

New biomaterials also interact with the tissue in specific ways at the molecular and cellular levels, combining the properties of bioabsorbability and bioactivity.

2.1. Bone tissue engineering (BTE)

Traditionally, trauma, osteonecrosis and tumour lesions have been treated with autologous, allogeneic or xenogeneic grafts. In certain cases, the implementation of substitute materials is needed. However, in view of serious problems such as donor scarcity, disease transmission, donor site morbidity and inability of materials to reshape and react to physiological conditions, BTE arises as an option to restore, maintain or improve functions through the creation of biological substitutes.

As previously explained, TE involves three fundamental elements: scaffolds, cells and biologically active molecules. According to Bose et al. [9] and Hutmacher et al. [10], the requirements for an ideal scaffold in case of osseous tissues are:

- Biocompatibility: to allow adequate integration into the host tissue without toxic effects (genotoxic or cytotoxic) and/or immune response.
- Porosity: to obtain open and interconnected pores to promote vascularization, to allow the diffusion of nutrients and gases, and to allow the removal of metabolic wastes as a result of cellular activity. Optimal pore size for BTE varies between 200 and 900 μm.
- Surface properties: both, chemical and topographic features control and affect cell adhesion and proliferation. The former are related to the ability of the cells to adhere to the material, whereas the latter are essential for osteoconduction. By this process, osteogenic cells migrate to the surface of the three-dimensional matrix through a fibrin clot, which is set after scaffold implantation.
- Osteoinductivity: to induce osteogenesis, *i.e.* mother and osteoprogenitor cells are recruited at the site of regeneration and stimulated to be differentiated into new bone.
- Mechanical properties: they depend on the site of implantation and the acting mechanical forces.
- Biodegradability: to allow materials to degrade *in vivo* at a controlled resorption rate that equals the bone formation rate, so that when the lesion is fully regenerated, the three-dimensional matrix has completely degraded.
- Radiolucency: to allow materials to radiographically differentiate the new bone from the implanted material. This allows one to efficiently evaluate the tissue regeneration.

3. Additive manufacturing techniques for scaffold fabrication

Numerous techniques have been developed to manufacture two- and three-dimensional scaffolds. The main technique to manufacture two-dimensional scaffolds is electrospinning, see [11,12]; whereas the main techniques to manufacture three-dimensional scaffolds include solvent casting, freeze drying [13], particle/salt leaching [14,15], chemical/gas foaming [16], thermally induced phase separation [10] and the foam-gel technique [17]. All these techniques have restrictions to produce scaffolds with specific micro-architectures in terms of porosity, pore size, pore geometry and interconnectivity. Moreover, due to their manufacturing conditions, these techniques do not allow including living cells or soluble factors within the process [18]. However, they are still being used because of their low cost and minimal equipment complexity.

AM techniques have arisen as a solution to the aforementioned disadvantages of the traditional manufacturing methods. They were introduced by Chuck Hull in 1986 [19] with a process known as Stereolithography (SLA). Over the last years, these methods have been widely discriminated, becoming more accepted in the scaffolds fabrication.

Other commercially available AM procedures are Selective Laser Sintering (SLS) [20], melt extrusion or Fused Deposition Modeling (FDM) [21] and Three-Dimensional Printing (3DP). The latter was developed and published as a patent by the Massachusetts Institute of Technology (MIT) in 1994, see [22]. Nowadays, this technique has become the most popular.

All the above mentioned techniques consist in obtaining of a layer-by-layer composition from a three-dimensional Computer-Aided Design (CAD) model, which achieves great precision, resolution, and reproducibility. Moreover, they allow the integration with medical imaging systems to obtain customized models and, in some cases, the incorporation of biomolecules or drugs.

Table 1 presents a brief description of these AM techniques, particular descriptive parameters in terms of layer thickness and resolution level, main advantages and disadvantages regarding scaffold manufacturing properties as well as the corresponding literature references. The table also shows the relative accuracy and costs, by the indicators sign (+) and ($), respectively (in a 1 to 3 scale).

The following sub-sections describe in detail the main characteristics, applications, evolution process and useful materials of each of these AM techniques.

3.1. Stereolithography (SLA)

This technique uses an ultraviolet light or laser to selectively polymerize layers of a photosensitive polymer. The stages to obtain SLA printed models are (see [23,26]):

(1) Immersion of a platform in a photopolymer liquid.
(2) Exposure to light according to the desired design.
(3) Polymer solidification at the point/s exposed to light, whereas non-exposed polymer remains liquid.
(4) Layer by layer fabrication by moving the platform downwards until the three-dimensional object is finally completed.

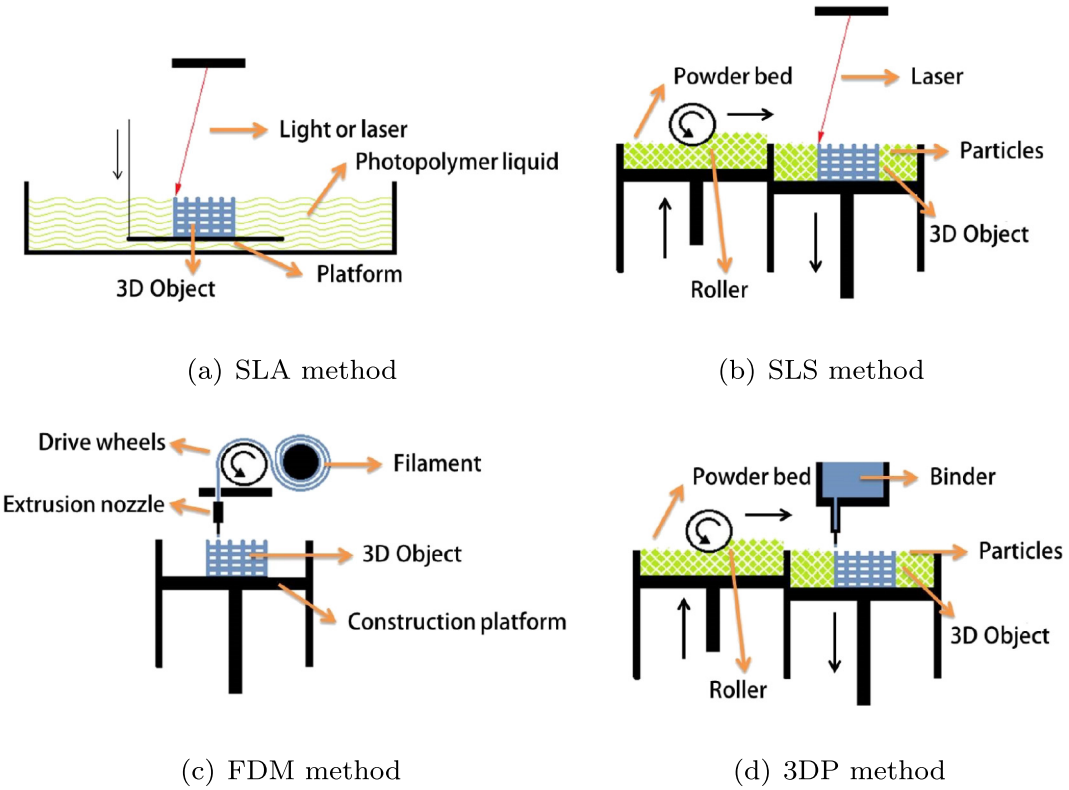

Fig. 1. Schematic representations.

(5) Removal of the non-polymerized resin.
(6) Post-curing of the green part improve the polymerization between layers and to reduce surface irregularities.

These stages are schematized in Fig. 1.

This technology, which is based on the use of UV light and photosensitive polymers, allows the highest resolution among all the AM techniques. The average resolution is approximately 150 μm. In addition, it should be noted that it has already been improved by the microstereolithography technique, which allows reaching resolutions of 0.5 to 10 μm, see among others [29–31,32]. Fig. 2 shows scaffolds manufactured by the SLA technique.

The main disadvantage of the SLA technique is the production of three-dimensional models only from the photosensitive polymers or composites containing them. Since, in the past, these materials were non-biocompatible and non-biodegradable, this technique was not applicable to TE. Therefore, some researchers used the indirect fabrication of scaffolds. For example, in 1999, Levy et al. [33], a suspension made of a photocurable acrylic resin mixed with Hydroxyapatite (HA) powder as a precursor of the SLA process. Then, the object obtained was subjected to a heat post-processing, thereby the acrylic resin was removed and an HA porous structure was obtained. Latter, in 2001, Chu [34] applied another indirect process: an epoxy mold was infiltrated with a HA suspension in acrylate binders, afterwards the mold and the

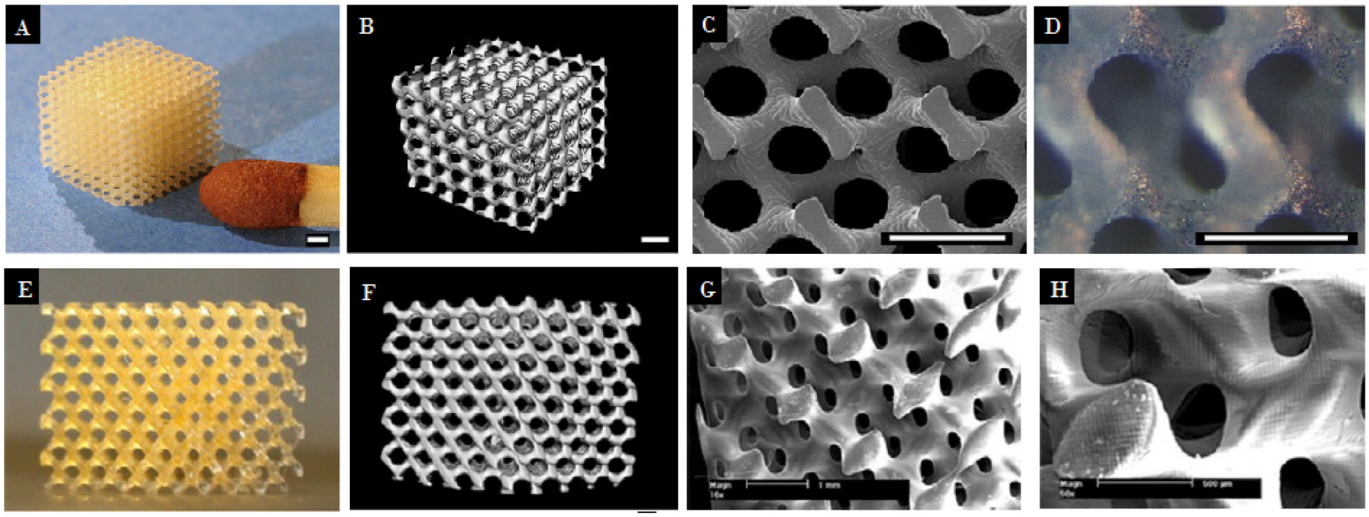

Fig. 2. Images of network scaffolds with a gyroid architecture, built by SLA. (A) Photograph. (B) μCT visualization. (C) SEM image. (D) Light microscopy images. In A, B, C and D: Scale bars represent 500 mm and are reprinted from Biomaterials Journal, 2009, ©Elsevier, all rights reserved. (E) Photograph. (F) μCT visualization. G and H SEM images (Scale bars represent 1 mm). In E, F, G and H are reprinted from Acta Biomaterialia Journal, 2011, ©Elsevier, all rights reserved.

binders were removed by pyrolysis, and a sintering process was performed.

The development of biodegradable structures by SLA was first reported by Matsuda et al. in 2000 [35]. However, the diversity of photocurable polymers with suitable properties for their application in TE is still limited, see [36]. As outlined by Dhariwala et al. [37] and Arcaute et al. [38], the possibility of encapsulating cells turned the SLA into a very promising technique with potential applications in regenerative medicine.

According to Mota et al. [26], the application of SLA techniques has some serious disadvantages, including: (i) the shrinkage of the structure during the production process and the post-processing step, (ii) the need, sometimes, for auxiliary supports (iii) the difficulty in loading the bioactive agents and multi-material structures. As an alternative to this last drawback, Choi et al. [39] have developed a multi-material stereolithography machine.

On the other hand, to reduce the manufacturing time, Dudley et al. developed a new SLA technique with a Digital Micromirror Device. In contrast to the 'point to point' light exposure, this procedure involves an array of several millions of mirrors that can be rotated independently to a 'on and off' state with the aim to project a two-dimensional pixel-pattern, see [40]. In consequence, a complete layer of resin can be cured at once, with the consequent reduction of time. In 2015, Tumbleston et al. [41] presented another alternative to reduce the manufacturing time by a continuous liquid interface production.

It should also be noted that a novel technique known as two-photon mSLA was proposed in 2007 by Ovsianikov et al. [42], to improve some of the fabrication aspects of polymeric porous structures by SLA, as the resulting resolution levels and manufacturing time. The desired object is manufactured directly inside the reactive medium without superimposition of layers by using a femtosecond laser. Resulting resolution sizes are below 100 nm [43] and the structures obtained present good *in vitro* cytocompatibility but lack biodegradability. The biodegradable materials available for this technique, include triblock co-polymer poly (e-caprolactone-*co*-trimethylenecarbonate)-b-poly(ethyleneglycol)-b-poly(e-caprolactone-co-trimethylenecarbonate) [44] and methacrylamide-modified gelatin (GelMOD) [45]. Materials commonly used for BTE scaffolds manufacture by SLA as well as the literature references to their application are listed in Table 2.

Recently, scaffolds made by two-photon mSLA of poly(D,L-lactide-*co*-β-caprolactone) copolymer with varying lactic acid and ϵ-caprolactone have been produced *via* ring-opening-polymerization and photoactivation. These scaffolds have a great potential in TE and regenerative medicine applications, see [46].

Table 2
Materials commonly used for BTE scaffolds by SLA.

Material	Reference
Poly(propylene fumarate) (PPF)/diethyl fumarate (DEF)	[29]
PPF	[30,32,47,48]
PPF/DEF-HA (hydroxyapatite)	[31]
Trimethylenecarbonate (TMC)/E-caprolactone (CL)	[49]
Poly(D, L-lactide) (PLA)	[50,51]
Poly(ethylene glycol) (PEG)	[32,37,38,52]
Polycaprolactone (PCL)	[53,54]
β-Tricalcium phosphate (β-TCP)	[55,56]
Poly(trimethylene carbonate) (PTMC)/nano-hydroxyapatite (nHA)	[57]
Polyethylene glycol diacrylate (PEGDA)	[58]
HA/poly(ethylene glycol) dimethacrylate (PEGDMA) and HA/PEGDA	[59]
HA/β-TCP/Agarose	[60,61]
HA/olygocarbonate dimethacrylate	[60]

3.2. Selective laser sintering (SLS)

SLS is based on small particles of thermoplastic, metal, ceramic or glass powders that are fused by a high power CO_2 or a Nd:YAG laser beam, see [24,62]. The following sequence must be followed to complete the formation of a three-dimensional body (Fig. 1):

(1) Preparation of the powder bed. For each layer, a new layer of powder is placed on top of the previous one.
(2) Exposure to light according to the desired design. For each layer, the selected particles are joined according to the CAD file using a laser.
(3) Removal of the remaining powder of the dissociated or non-sintered areas.

Fig. 3 shows scaffolds fabricated by the SLS technique. The mechanical properties and size accuracy of the scaffolds obtained are strongly dependent on the construction planes and processing parameters such as manufacturing direction, hatch distance, particle size, laser intensity and powder bed temperature, see among others [62–67]. Generally, SLS scaffolds present low mechanical properties, thus limiting their application to non-load-bearing sites, see [67,68,69].

The scaffold morphology can be controlled by several processing parameters:

- Powder **particle size** is preferred in the range of 10–150 μm, according to [70].
- The **laser energy density [J/cm^2]** follows from the melting point of the powders and can be set by adjusting the laser power, spot size of the beam and scan speed, see [71]. Decreasing the laser scanning speed, allows obtaining denser parts because of the longer interaction time between the powder and the laser beam, which boosts the rate of energy delivered to the powder bed, see [72]. Therefore, the laser energy density directly affects the object porosity. On the other hand, as outlined by Savalani et al. [71] and Amorim et al. [72], the smaller the layer thickness the stronger the bonding between the layers. This is because if the thickness of the powder layers is relatively low for the same laser settings greater fusion would occur due to the lesser material quantity and subsequent greater absorption of heat from the previous layer. This fact decreases the porosity of the pieces.
- **Hatch distance** also affects porosity. Shirazi et al. [62] recommend to choosing a hatch distance equal to or greater than the laser beam spot size to avoid overlapping and to obtain appropriate connectivity to the matrix.

In 2003, Tan et al. [73] developed one of the first scaffolds for BTE by SLS with polyetheretherketone and HA. Later, this technique was applied by Williams et al. [65] to fabricate porous polycaprolactone (PCL) scaffolds, with or without additional calcium phosphate particles. The mechanical properties of these scaffolds were within the order of the range of trabecular bones. Afterwards, nanostructured materials introduced by Shuai et al. [74] and Zhou et al. [75] evidenced, good potential for TE applications. Moreover, [68,76–79] performed several studies on poly(hydroxybutyrate-*co*-hydroxyvalerate) tricalcium phosphate (PHBVTCP) scaffolds by applying SLS to composite microspheres. In all cases, the addition of different components improved the bioactivity of the scaffolds.

Indirect fabrication of scaffolds was also reported. In the case of bioglass, stearic acid is used as a binder and then removed to obtain a final object as mentioned by Kolan et al. [63,69]. Some scaffolds, on the other hand, are built using natural components as cellulose or different polysaccharides, see Salmoria [64] and Ciardelli et al. [66] respectively.

Recently, Liao et al. [80] have fabricated PCL-TCP scaffolds *via* SLS. They coated collagen type I (COL) and obtained PCL-TCP-COL scaffolds,

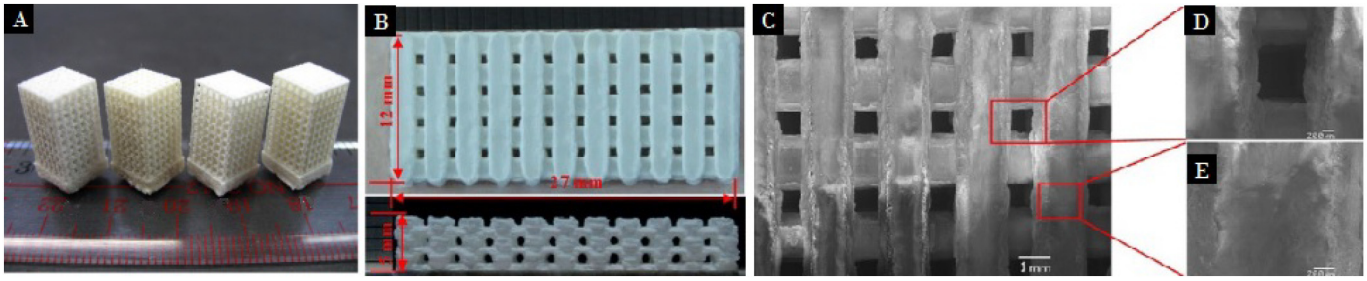

Fig. 3. Images of scaffolds built by SLS. (A) Photograph reprinted from Acta Biomaterialia Journal, 2010, ©Elsevier, all rights reserved. (B) Photograph. (C), (D) and (E) SEM images are reprinted from Scientific reports Journal, 2009, ©Nature Research, is licensed under a Creative Commons Attribution-NonCommercial-ShareAlike 4.0 International License. To view a copy of this license, visit http://creativecommons.org/licenses/by-nc-sa/4.0/.

with good results.

It should also be noted that many scaffolds are composed of polymer and ceramic composites. The ceramic content of the composites strongly affects the mechanical properties and degradation behaviour and it must be considered as a critical design parameter, see [81].

In 2014, Feng et al. [82] proposed another new strategy to improve the general characteristics of scaffolds, named Novel Two Step Sintering (NTSS). This approach includes two steps: a first step conducted by SLS using a laser characterized by the rapid heating to skip the surface diffusion, and a second step that consists in isothermal heating in a furnace at low temperature to increase the final density.

Table 3 summarizes the materials commonly used to obtain BTE scaffolds by SLS and the corresponding literature references.

3.3. Fused deposition modelling (FDM)

FDM is based on the extrusion of a polymeric filament through a heated nozzle. As shown in Fig. 1, a three-dimensional object can be obtained following these steps:

(1) The filament is supplied to the extrusion nozzle by means of drive wheels.
(2) The polymer is heated in the extrusion nozzle until it melts.
(3) Polymer melt is continuously deposited on a construction platform.
(4) The extruder head is computer-controlled and builds layer by layer the three-dimensional object layer by layer.

Table 3
Materials commonly used for BTE scaffolds by SLS.

Material	Reference
Polymers starchcellulose and cellulose acetate	[64]
13–93 bioactive glass using stearic acid	[63,69]
HA/Polyamide-12	[71]
Calcium phosphate (CP)/poly(hydroxybutyrateco-hydroxyvalerate) (PHBV)	[70]
Carbonated hydroxyapatite (CHAp)/poly(ι-lactic acid) (PLLA)	[70]
Polycaprolactone (PCL) (with or without additional CP particles)	[65,83]
Nano HA	[74]
PLLA	[84]
Poly (3-hydroxybutyrate) (PHB)	[85]
(PCL)/polysaccharide (starch, S; dextran, D; or gellan, G)	[66]
HA/PCL	[67,73,86,87]
Poly(hydroxybutyrate-co-hydroxyvalerate) (PHBV) microspheres and CaP/PHBV	[68]
Polyetheretherketone (PEEK)/HA	[73,88]
PCL/nanoHA	[75]
PLLA/HA	[89]
PEEK/poly (glycolic acid) (PEG)	[90]
Poly[3,6-dimethyl-1,4-dioxane-2,5-dione]/HA	[91]
PCL/-TCP	[81]
PVA	[92]
Aliphatic-polycarbonate/HA a-PC/HA	[93]
PLLA/β-TCP	[94]
PCL/TCP/collagen type I (COL)	[80]

(5) The layer thickness is determined by the movement downwards of the construction platform.

As stated by Houben et al. [95], FDM can generate structures with strut diameters in the range of several hundred micrometers which are mainly controlled by the nozzle diameter and the extrusion rate. The resolution given by an FDM manufacturing equipment is affected by several parameters which will define the quality of the resulting scaffold. Some of these parameters are:

- The coordination between the head movements and the drive wheels that provided by the material.
- The heat retained in the material after being deposited, which may cause non-controlled deformations.
- In case of discontinuous scaffolds, the movement of the extrusion nozzle from the last filling point to the next, may produce unwanted filaments.

The range of appropriate materials for FDM remains limited since they must satisfy the following properties: (i) thermoplasticity, (ii) suitable viscoelasticity, (iii) melting/solidification, and (iv) ability to be pre-processed into polymer filaments.

Recently, Probst et al. [96], Jiang et al. [97] and Pati et al. [98] proposed preparing some composites using PCL as thermoplastic counterpart to use FDM. As it is known, PCL scaffolds are able to support *in vitro* proliferation, differentiation and extra cellular matrix production of primary human fibroblasts and periosteal cells [99]. Rohner et al. [100], for example, reported 14,1% formation of new bone in a pig model after three months, by using PCL scaffolds with bone marrow coated prepared by FDM. Due to the favourable results of this biomaterial and the low manufacturing costs, several clinical studies have been carried out and the US Food and Drug Administration (FDA) has approved the application of PCL scaffolds made by FDM in humans, see [101,102]. These are currently commercialized by Osteopore Pte. Ltd. in the form of thin interwoven meshes (Osteomesh™) and three-dimensional implants (Osteoplug™). As previously stated, FDM application is so far limited to a few thermoplastic polymers because it can only use filament-shaped materials. To process a wider range of polymeric materials in diverse forms (*e.g.* pellet, powder), a melt extrusion-based technique was developed, see [26]. The most popular in TE is the three-dimensional fibre deposition (3DF) technique, also called three-dimensional plotting or Air pressure Jet Solidification. This procedure applies air pressure instead of rollers to force solutions or melts through a nozzle. This allows applying a larger range of materials, including hydrogels, polymer/ceramic sludges, *etc.* Similarly to FDM, strut diameters are in the range of several hundreds of micrometers. A 3DF system with the trademark 3D-Bioplotter is currently marketed by EnvisionTEC GmbH. Another well-known 3DF system is BioScaffolder, commercialized by GeSiM mbH. As an alternative for the multi-material pieces, some researchers as Kang et al. [103] have presented a multi-material printer that combines FDM and 3DP.

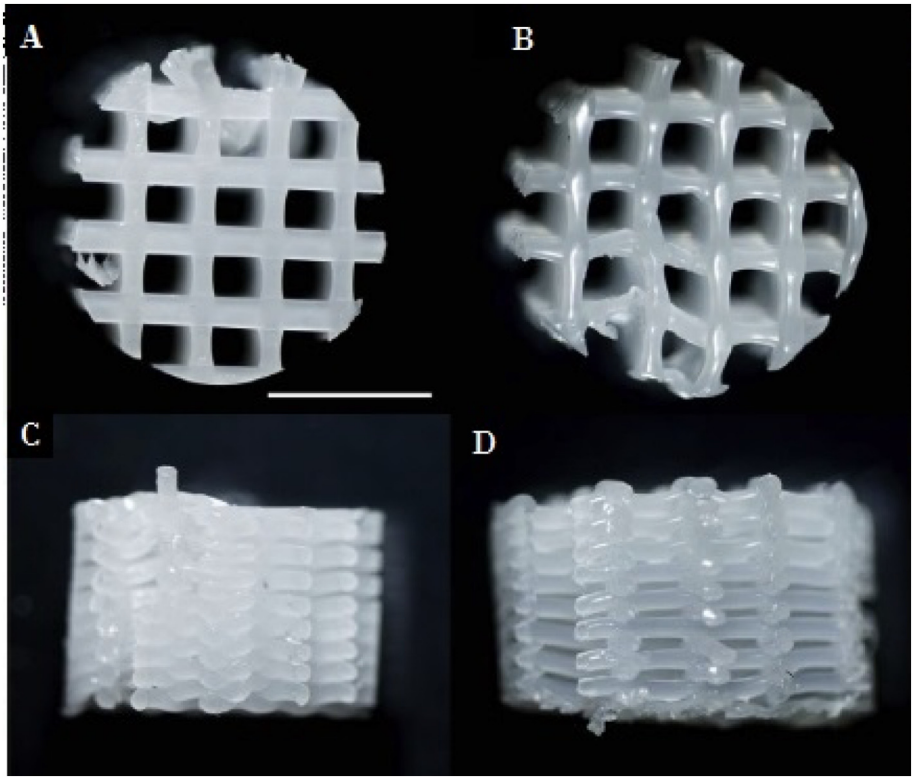

Fig. 4. Images of scaffolds built by FDM. Photograph: (A) Top view of PCL scaffold. (B) Top view of PHMGCL scaffold. (C) Side view of PCL. (D) Side view of PHMGCL scaffold. Scale bar 2.5 mm. Reprinted from Biomaterials Journal, 2012, copyright Elsevier, all rights reserved. Stereomicroscopic images of pHMGCL scaffold: (E) and (F) Side views. (G) Top view. (H) Oblique view. Scale bar 1 mm. Reprinted from Acta Biomaterialia Journal, 2011, ©Elsevier, all rights reserved. Normal size.

Some researchers have used this method for the indirect fabrication of scaffolds. B'egin-Drolet et al. [104], for example, described the use of sugar glass as the ink to create a vascular network used as a mold for scaffolds of polydimethylsiloxane (PDMS).

A broad spectrum of biomaterials such as calcium phosphate ceramics and cements, bioglasses, synthetic polymers such as poly(ϵ-caprolactone) and biopolymers including starch and chitosan, have been applied for 3DF scaffolds. Fig. 4 shows scaffolds manufactured with the FDM technique.

Hydrogels are very popular within the TE field because living cells can be added on their surface under mild processing conditions. Some hydrogels are: agar, agarose, collagen, gelatin, alginate, mixtures of alginate and gelatin, and Lutrol F127, see [105]. Recently, a large number of photopolymerizable hydrogels have been developed and applied for the plotting of cell-laden scaffolds. However, hydrogels are not used in BTE because of their limited mechanical properties. They can be used to develop composites together with some tough materials that provide the required strength.

It is possible to use more than one material by introducing extrusion syringes, either in FDM or 3DF. Jiang et al. [97] have developed a 3DF-system with two syringes, one for a biocomposite and the other for a biopolymer, using PEG and PCL with nano-HA.

Giron et al. [106] used on the combination of 3DF and pipetting, which enables the creation of scaffolds with complex patterns of functional substances. The resolution of the pipetting is generally excellent. With integrated pipetting, the range of materials that may be seeded with live cells can be widened, because the cells should not be immersed in the plotting pastes. Furthermore, the pipetting allows tailoring the local concentrations of drugs or biological factors (or the cell seeding density) unlike the homogeneous distribution provided by mixing the plotting paste with the substance or cells, respectively.

The materials useful for BTE scaffolds and the corresponding references are listed in Table 4.

Table 4
Materials commonly used for BTE scaffolds by FDM and 3DF.

Technique	Material	Reference
FDM	PCL	[99,100]
	PLA	[107,108]
	PCL/TCP	[96]
	PCL - PCL/bTCP	[109]
	PP-TCP	[110]
33DF	PEG and PCL with nano HA	[97]
	PCL/PLGA and PCL/PLGA/TCP	[98]
	PCL and poly(hydroxymethylglycolide-co-e-caprolactone) (PHMGCL)	[111]
	PHMGCL	[112]
	HA-forming calcium phosphate cements	[113]
	PCL	[114,115]
	HA	[116]
	Calcium phosphate cement	[117]
	6P53B bioglass	[118]
	Mesoporous bioactive glass	[119]
	Starchpolycaprolactone	[120]
	PLA/chitosan	[121]
	Agarose (H), alginate (H) or Lutrol F127. gelatin (H)	[122]

3.4. Three-dimensional printing (3DP)

This method is based on the controlled deposition of a binder material laid on a powder by using an ink-jet head. A three-dimensional object is obtained with the following steps (see Fig. 1):

(1) Preparation of the powder bed.
(2) For each layer, the binder is selectively deposited according to a CAD file. This binder joins, which consists of an organic or aqueous solution that cannot only wet the surrounding powder, but can also locally harden the wetted area, joins the powder particles.
(3) A new powder bed is added and spread mechanically layer by layer by using a roller on top of the previous one.
(4) The layer by layer process goes on until the three-dimensional

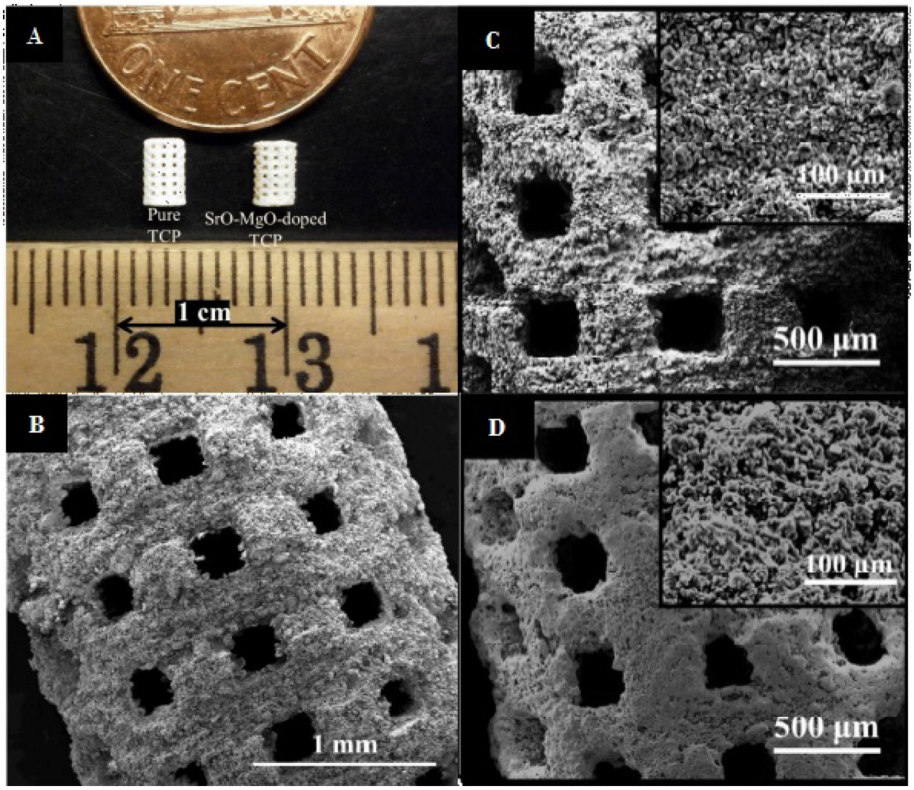

Fig. 5. Images of scaffolds built by 3DP. (A) Photograph. (B) SEM image. (A) and (B) are reprinted from Biomaterials Science Journal, 2013, ©Royal Society of Chemistry, all rights reserved. (C) TCP scaffold. (D) Surface morphology of PCL coated TCP scaffolds. (C) and (D) are reprinted from ACS Publications: Applied Materials & Interfaces Journal, 2014, ©Elsevier, all rights reserved.

object is finally built.
(5) The unbound powder that composes each layer acts as support for the object being built. Finally, this powder is removed.
(6) In general, it requires a post-processing step with heat.

In this technique the scaffold quality is defined by the following properties:

- Powder flowability: this is an essential requirement for building up thin powder layers and removing the powder from the printed part. Flowability is primarily determined by particle size, size distribution, surface roughness and shape. High flowability allows the roller to build up thin and homogeneous layers and thus enables higher resolution in the printed solid. Resolution is generally at least twice the dimension of the powder particle size [123]. However, fine powder (dry) can agglomerate due to attractive interactions between spherical particles (Van der Waals forces) that can dominate gravitational forces and reduce flowability, resulting in poor compaction and unacceptable powder bed re coating. However, according to Butscher et al. [124], subjecting fine powder to plasma treatment allows the increment of interparticle distance, reducing the Van der Waals forces and improving flowability. Therefore, a trade-off between flowability and resolution is inevitable. Low flowability makes depowdering after printing a difficult and sometimes unachievable goal. Depowdering of simple cavities demands a minimum cavity diameter of five times the average powder size [125]. This value might be even higher for complex cavity systems and irregular cellular structures [27].
- Particle size: the importance of particle size in the success of a 3DP process was confirmed by Zhou et al. [126]. Fine powders ($\leq 20\,\mu m$) resulted in slow drop penetration speed, large drop penetration depth, low wetting ratio, poor green mass and green strength for the final 3DP components. The optimal particle size for a good printability ranges from 20 to 35 µm [124], while the recommended particles shapes are spherical [127].
- Binder drop volume: the binder drop volume is the amount of binder released from each nozzle per drop during printing, which depends on the density and viscosity of the binder. This parameter affects the binder saturation.
- Layer thickness: thinner layers allow the binder to bleed through other sites not selected by the CAD file resulting in poor resolution and tolerance. However, a thicker layer requires high saturation, which also leads to the same problem. Binder bleeding causes the blocking of the designed pores [128].
- Powder packing density: the powder packing density is the relative density of the powder bed after uniform spreading.
- Binder saturation: coordinating the powder packing density and the drop volume, allows obtaining the binder saturation data required for printing. A high drop volume requires a low saturation and vice versa. Saturation could vary according to layer thickness and powder morphology. A thicker layer would require relatively high saturation [128]. The binder saturation also depends on the powder wettability.
- Powder wettability: the powder wettability depends on many parameters, such as the contact angle between the binder and the powder, the binder viscosity, the topography of the powder bed surface (which in turn on the powder shape and size) and the chemical reactions occurring between binder and the powder [27]. This factor determines the printing accuracy and the achievable tolerance [23]. High wettability results in extensive binder spreading, limiting the printing resolution, whereas results in poor joints between neighbouring printed layers and thus low mechanical integrity of the object [129].

A remarkable advantage of 3DP is its ability to process a large variety of ceramic, metallic, polymeric and composite materials. The only condition is the availability of the material in a powder form. However, binder selection and process parameter optimization are the keys to success in fabrication. The materials so far investigated for BTE scaffolds include polymeric, ceramic and composite powder materials [28].

The most employed materials are bioactive ceramics such as HA,

Table 5
Materials, binders and some parameters used for BTE scaffolds by 3DP.

Material	Binder	Layer thickness	Particle size	Porosity	Post-processing	Ref.
HA	94.5% water two times distilled, 2.5% glycerin, 3.0% others	50 μm	4 μm, 50 μm	NI	1 °C/min to 600 °C 3 °C/min to 400 °C	[133]
β-TCP, β-TCP/ZnO/SiO_2	Commercial organic water based (ProMetal)	20 μm	30–550 nm	32–52%, 32–46%	1250 °C for 2 h	[134]
TCP, HA, BioOss™	Dextrin, saccharose	250 μm	NI	Pore size: 480 μm	1250 °C for 2 h	[135]
HA, TCP, HA/TCP (60:40)	Dextrin 20 wt%, saccharose 2,5 wt%	260–290 μm	32–36 μm, 52–57 μm, 37–42 μm	35% macro 60% micro	1250 °C for 2 h	[127]
HA, TCP, HA/TCP (60:40)	Dextrin 20 wt%, saccharose 2,5 wt%	100 μm	32–36 μm, 52–57 μm, 37–42 μm	52–56% Pore size: 5–200 μm	1300 °C for 1 h	[136]
HA	Water based polymer	240 μm	22 μm	67.2%, 70.3%	1250 °C for 2 h	[137]
TCP, TCP/HA	Phosphoric acid 10% and 20%	100 μm	NI	29%, 59%	Immersion in H_3PO_4 and Na_2HPO_4 at 37 °C	[138,139]
PLGA	Ethanol, acetone and de-ionized water	NI	100 μm	50% Pore size: 1 mm	Leached with an ultrasonic cleaner and the remaining portion was annealed	[140]
50 wt% cornstarch, 30 wt% dextran and 20 wt% gelatin	Water based	NI	NI	Pore size: 2.5 mm	100 °C for 1 h	[132]
Collagen-calcium phosphate composites	Dilutions of phosphoric acid (5e20 wt%) with Tween 80 (Sigma-Aldrich, St. Louis, MO) 0.25 wt%	89 μm	30–150 μm	22%–35%	1300 °C for 2 h	[141]
HA, β TCP and potato starch (35:35:30)	NI	NI	NI	Pore size: 52 μm	1200 °C and coated with collagen 0.01%	[142]
HA and maltodextrin	Water based	175 μm	3–5 μm	59–65%	1300 °C for 3 h	[143]
TTCP/β TCP (30:70)	25% citric acid in distilled water	100 μm	< 100 μm	~38%	1000 °C–1400 °C for 6 or 24 h	[144]
β TCP	510% phosphoric acid	100 μm	30 μm	38%–42%	Immersing in 20% phosphoric acid for 30 s drying in air for 1 h. 1100 °C and 1300 °C for 5 h	[145]
HA 14%	Schelofix64 in water	NI	69 μm (d50)	NI	NI	[?]
HA and maltodextrin/apatitewollastonite glass	Water-based	100 μm	35 μm and 90100/88 μm (d50)	Depends on sintering temperature	1050, 1200 and 1300 °C for 1 to 10 h	[146]
CP (calcium polyphosphate)/PVA	Zb 58 10 wt% PVA	150 μm	75150 μm	~35%	A sintering in two steps	[147]
TCP and calcium carbonate	10 v/v% phosphoric acid	112 μm	< 100 μm	6368%	1200 °C for 5, 10 or 15 h	[148]

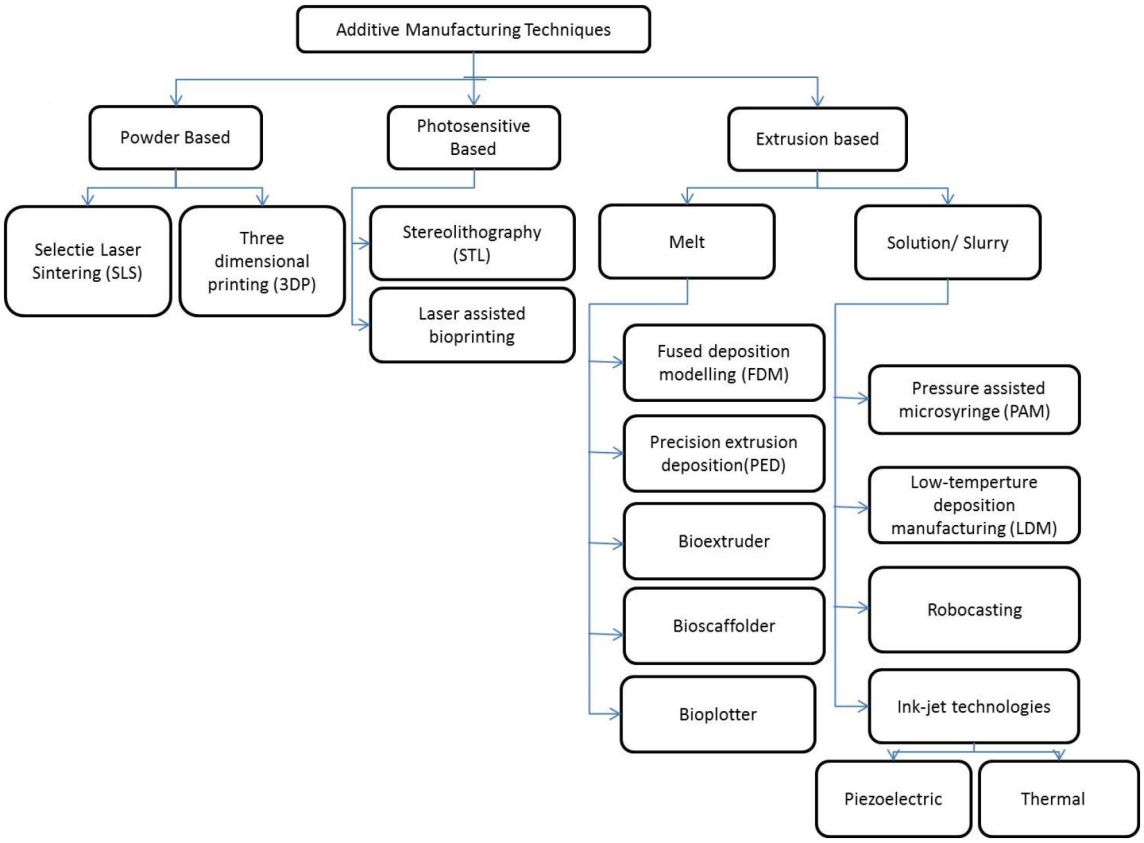

Fig. 6. Proposed general classification of the AM techniques commonly employed in TE.

bioactive glasses and tricalcium phosphates (TCP), see [130,131] and [128]. Natural polymers have also been proposed but in general, they presented limited structural integrity and low mechanical properties [132]. Fig. 5 show scaffolds fabricated by the 3DP technique.

To enhance the binding properties of ceramic particles, Shanjani et al. [147] developed a novel 3DP technique involving the processing of a polymer-ceramic mixture followed by the elimination of the polymer phase after sintering.

Table 5 summarizes the different materials, binders, layers thickness, particles sizes, porosity and details of post-processing used in the field of BTE by 3DP, as well as the corresponding references.

Among the main disadvantages of 3DP, it is worth noting the need of post-processing steps (*e.g.* sintering) to improve the resulting mechanical properties. Sintering produces shrinkage, which causes distortions and fracture [147] and thus, precludes the addition of biomolecules inside. In case of low temperature 3DP (without post-processing with heat), powder solidification is carried out *via* a hydraulic setting reaction [149]. Furthermore, as no thermal treatment is required, so it enables the incorporation of bioactive molecules and drugs during the 3DP process. This is best exemplified by Gbureck et al. [150] who investigated scaffolds with drug delivery.

Similarly to observed in the SLS technique, other drawbacks of the 3DP process are the residual non-bound material in complex geometries and possibly highly rough surfaces [27]. Last, can also be considered as a disadvantage because organic solvent binders will dissolve printhead subsystems, commercially available [151].

Lee et al. [151] and Tamjid et al. [152] have applied an alternative procedure, called Indirect 3DP. This approach consists in: (i) a positive replica of desired shapes is printed using any material, and (ii) producing the final the commonly used synthetic biodegradable polymers scaffold by using a biodegradable polymer solution cast into the printed mold cavity. This strategy avoid the use of organic solvent as binder, needed in case of biodegradable materials, although it does not allow obtaining well-defined complex internal architectures because of the difficulty of removing the mold from the internal pores.

3.5. Other AM techniques

Over the last three decades, AM techniques applicable to many research areas have boomed around the world. New practices and variations of the existing ones are constantly emerging. This fact, added to the variety of denomination used by the different authors, makes it very difficult to enumerate them. In addition, as there is no standardized classification, a general classification of the most recognized techniques is proposed in Fig. 6.

It should be noted that some researchers, as Ragelle et al. [153] have combination of different methods to obtain novel improvements.

4. Discussion

AM techniques are very promising for the manufacture of BTE scaffolds. However, there present both advantages and disadvantages and certain design parameters that are decisive when choosing a specific technique. The choice is defined by the micro-architecture characteristics, biocompatibility and biodegradability of the materials, as well as by their accessibility, in terms of simplicity of application and low cost.

Regarding the micro-architecture, two main characteristics can be mentioned, framework and porosity. For both, the reached resolution will be crucial to achieve the correct sizes. The recommended pore size for BTE scaffolds lies between 200 μm and 900 μm. Then the resolution level, which depends both on the technique used and the specific equipment, must be sufficient to reach these values.

SLA has the smallest resolution. Therefore, it allows obtaining pore sizes of 200 μm, as SLS. In contrast, FDM and 3DP, allow obtaining pores smaller than 900 μm, particularly from 250 μm–700 μm with FDM

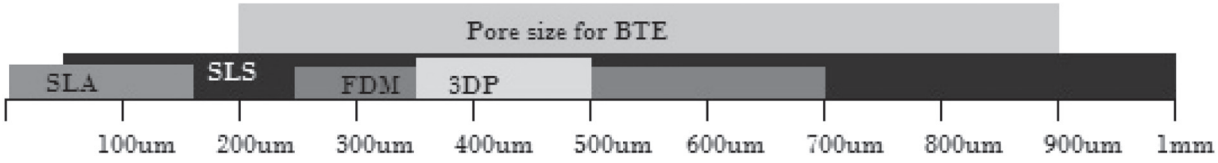

Fig. 7. Comparison of resolution ranges.

and from 350 μm–500 μm to with 3DP. It should be pointed out that these are average values and that are some particular cases of values away from these ranges. Fig. 7 shows the ranges of resolutions that can be handled with the different methods.

Another essential feature for the manufacture of BTE scaffolds is the selection of a suitable biomaterial, since properties such as biocompatibility and biodegradation are inherent. In the case of SLA, the variety of photopolymerizable materials suitable for TE applications is still limited. For this reason, this technique is still not widely used for BTE applications. Likewise the SLS method is considered inadequate due to the high intensity of the applied laser, which generally degrades the polymer. Its use is very limited and quite expensive. For these reasons, the mentioned technologies, despite having the best resolution, are not the best options to produce biodegradable scaffolds.

As described in Section 3, the applicable materials by FDM are limited because they must be thermoplastic, with a suitable viscoelasticity and melting/solidification properties as well as the ability to be pre-processed into polymer filaments. However, it should be noted that the FDA has approved a method for the manufacture of PCL scaffolds. 3DF is a variation of the FDM, in which a wide range of biocompatible and biodegradable materials can be used, with the advantage of having specific equipment of relatively easy access, such as the 3D Bioplotter and Bioscaffolder. In addition, manufacturing parameters such as temperature and extrusion speed can be selected by the user and software-controlled. This fact simplifies the optimization process.

In the case of 3DP, a large variety of ceramic, polymers and composites bio-materials can be used. But, in this case, both a good selection of the binder and the optimization of several parameters, such as powder bedding, particle size and binder wettability, are required for a successful manufacture. This optimization demands an intensive work and is time-consuming.

Thus, according to the specific needs of the user, one technique may be more convenient than others. Regarding the accessibility in terms of the combination of simplicity, low cost and enough resolution, the FDM method is more convenient than others. Regarding, the manufacture of scaffolds with addition of stem cells, Chapelin et al. [154] stated that, in the future, it will probably decrease due to the risks of tumours formation. Finally, it is important to highlight that, regarding the incorporation of biomolecules, 3DF is the most adequate of the techniques presented in this review.

The analyses and comparisons made in this review, allow concluding that all techniques have a wide potential in BTE applications in the following fields, especially if they are accompanied by progress:

- Design of the micro- and macro-structure of scaffolds, in terms of new frameworks or combination of existing ones with the aim to improve the tissue response.
- Design of new biomaterials to be specifically adapted to certain techniques to extend the range of applicable biomaterials.
- Combination of existing techniques to improve their applicability and create advances.

References

[1] V. Mouriño, A.R. Boccaccini, Bone tissue engineering therapeutics: controlled drug delivery in three-dimensional scaffolds, J. R. Soc. Interface 7 (2010) 209–227.
[2] A.C. Jones, C.H. Arns, A.P. Sheppard, D.W. Hutmacher, B.K. Milthorpe, M.A. Knackstedt, Assessment of bone ingrowth into porous biomaterials using micro-ct, Biomaterials 28 (15) (2007) 2491–2504.
[3] J.P. Schmitz, J.O. Hollinger, The Critical Size Defect as an Experimental Model for Craniomaxillofacial Nonunions, Tech. Rep, Walter Reed Army Medical Center, Washington DC, 1985.
[4] J. Mano, G. Silva, H.S. Azevedo, P. Malafaya, R. Sousa, S. Silva, L. Boesel, J.M. Oliveira, T. Santos, A. Marques, et al., Natural origin biodegradable systems in tissue engineering and regenerative medicine: present status and some moving trends, J. R. Soc. Interface 4 (17) (2007) 999–1030.
[5] S. Maietta, T. Russo, R. De Santis, D. Ronca, F. Riccardi, M. Catauro, M. Martorelli, A. Gloria, Further theoretical insight into the mechanical properties of poly-caprolactone loaded with organic–inorganic hybrid fillers, Materials 11 (2) (2018) 312.
[6] T. Patrício, M. Domingos, A. Gloria, U. D'Amora, J. Coelho, P. Bártolo, Fabrication and characterisation of pcl and pcl/pla scaffolds for tissue engineering, Rapid Prototyp. J. 20 (2) (2014) 145–156.
[7] V. Guarino, A. Gloria, M.G. Raucci, R. De Santis, L. Ambrosio*, Bio-inspired composite and cell instructive platforms for bone regeneration, Int. Mater. Rev. 57 (5) (2012) 256–275.
[8] R. Landers, U. Hübner, R. Schmelzeisen, R. Mülhaupt, Rapid prototyping of scaffolds derived from thermoreversible hydrogels and tailored for applications in tissue engineering, Biomaterials 23 (23) (2002) 4437–4447.
[9] S. Bose, M. Roy, A. Bandyopadhyay, Recent advances in bone tissue engineering scaffolds, Trends Biotechnol. 30 (10) (2012) 546–554.
[10] D.W. Hutmacher, Scaffolds in tissue engineering bone and cartilage, Biomaterials 21 (24) (2000) 2529–2543.
[11] H. Yoshimoto, Y. Shin, H. Terai, J. Vacanti, A biodegradable nanofiber scaffold by electrospinning and its potential for bone tissue engineering, Biomaterials 24 (12) (2003) 2077–2082.
[12] X. Liu, P.X. Ma, Polymeric scaffolds for bone tissue engineering, Ann. Biomed. Eng. 32 (3) (2004) 477–486.
[13] N. Sultana, M. Wang, Fabrication of ha/phbv composite scaffolds through the emulsion freezing/freeze-drying process and characterisation of the scaffolds, J. Mater. Sci. Mater. Med. 19 (7) (2008) 2555.
[14] M. Stoppato, E. Carletti, V. Sidarovich, A. Quattrone, R.E. Unger, C.J. Kirkpatrick, C. Migliaresi, A. Motta, Influence of scaffold pore size on collagen i development: a new in vitro evaluation perspective, J. Bioact. Compat. Polym. 28 (1) (2013) 16–32.
[15] H. Cao, N. Kuboyama, A biodegradable porous composite scaffold of pga/β-tcp for bone tissue engineering, Bone 46 (2) (2010) 386–395.
[16] M. Kucharska, B. Butruk, K. Walenko, T. Brynk, T. Ciach, Fabrication of in-situ foamed chitosan/β-tcp scaffolds for bone tissue engineering application, Mater. Lett. 85 (2012) 124–127.
[17] H. Yoshikawa, N. Tamai, T. Murase, A. Myoui, Interconnected porous hydroxyapatite ceramics for bone tissue engineering, J. R. Soc. Interface 6 (2009) S341–S348.
[18] R.F. Pereira, P.J. Bártolo, 3d photo-fabrication for tissue engineering and drug delivery, Engineering 1 (1) (2015) 090–112.
[19] C. W. Hull, Apparatus for production of three-dimensional objects by stereolithography, US Patent 4,575,330 (Mar. 11 1986).
[20] C. R. Deckard, Method and apparatus for producing parts by selective sintering, US Patent 4,863,538 (Sep. 5 1989).
[21] S. S. Crump, Apparatus and method for creating three-dimensional objects, US Patent 5,121,329 (Jun. 9 1992).
[22] E. M. Sachs, J. S. Haggerty, M. J. Cima, P. A. Williams, Three-dimensional printing techniques, US Patent 5,204,055 (Apr. 20 1993).
[23] S. Bose, S. Vahabzadeh, A. Bandyopadhyay, Bone tissue engineering using 3d printing, Mater. Today 16 (12) (2013) 496–504.
[24] F. Rengier, A. Mehndiratta, H. von Tengg-Kobligk, C.M. Zechmann, R. Unterhinninghofen, H.-U. Kauczor, F.L. Giesel, 3d printing based on imaging data: review of medical applications, Int. J. Comput. Assist. Radiol. Surg. 5 (4) (2010) 335–341.
[25] C.M.B. Ho, S.H. Ng, Y.-J. Yoon, A review on 3d printed bioimplants, Int. J. Precis. Eng. Manuf. 16 (5) (2015) 1035–1046.
[26] C. Mota, D. Puppi, F. Chiellini, E. Chiellini, Additive manufacturing techniques for the production of tissue engineering constructs, J. Tissue Eng. Regen. Med. 9 (3) (2015) 174–190.
[27] A. Butscher, M. Bohner, S. Hofmann, L. Gauckler, R. Müller, Structural and material approaches to bone tissue engineering in powder-based three-dimensional printing, Acta Biomater. 7 (3) (2011) 907–920.
[28] S.H. Jariwala, G.S. Lewis, Z.J. Bushman, J.H. Adair, H.J. Donahue, 3d printing of personalized artificial bone scaffolds, 3D Printing and Additive Manufacturing 2 (2) (2015) 56–64.
[29] P.X. Lan, J.W. Lee, Y.-J. Seol, D.-W. Cho, Development of 3d ppf/def scaffolds using micro-stereolithography and surface modification, J. Mater. Sci. Mater. Med. 20 (1) (2009) 271–279.

[30] J.-W. Choi, R. Wicker, S.-H. Lee, K.-H. Choi, C.-S. Ha, I. Chung, Fabrication of 3d biocompatible/biodegradable micro-scaffolds using dynamic mask projection microstereolithography, J. Mater. Process. Technol. 209 (15) (2009) 5494–5503.
[31] J.W. Lee, G. Ahn, D.S. Kim, D.-W. Cho, Development of nano-and microscale composite 3d scaffolds using ppf/def-ha and micro-stereolithography, Microelectron. Eng. 86 (4) (2009) 1465–1467.
[32] Y. Lu, G. Mapili, G. Suhali, S. Chen, K. Roy, A digital micro-mirror device-based system for the microfabrication of complex, spatially patterned tissue engineering scaffolds, J. Biomed. Mater. Res. A 77 (2) (2006) 396–405.
[33] R.A. Levy, T. Chu, J.W. Halloran, S.E. Feinberg, S. Hollister, Ct-generated porous hydroxyapatite orbital floor prosthesis as a prototype bioimplant, J. Neuroophthalmol. 19 (2) (1999) 113.
[34] T.-M. Chu, J. Halloran, S.J. Hollister, S.E. Feinberg, Hydroxyapatite implants with designed internal architecture, J. Mater. Sci. Mater. Med. 12 (6) (2001) 471–478.
[35] T. Matsuda, M. Mizutani, S.C. Arnold, Molecular design of photocurable liquid biodegradable copolymers. 1. Synthesis and photocuring characteristics, Macromolecules 33 (3) (2000) 795–800.
[36] D.W. Hutmacher, M. Sittinger, M.V. Risbud, Scaffold-based tissue engineering: rationale for computer-aided design and solid free-form fabrication systems, Trends Biotechnol. 22 (7) (2004) 354–362.
[37] B. Dhariwala, E. Hunt, T. Boland, Rapid prototyping of tissue-engineering constructs, using photopolymerizable hydrogels and stereolithography, Tissue Eng. 10 (9–10) (2004) 1316–1322.
[38] K. Arcaute, B.K. Mann, R.B. Wicker, Stereolithography of three-dimensional bioactive poly (ethylene glycol) constructs with encapsulated cells, Ann. Biomed. Eng. 34 (9) (2006) 1429–1441.
[39] J.-W. Choi, H.-C. Kim, R. Wicker, Multi-material stereolithography, J. Mater. Process. Technol. 211 (3) (2011) 318–328.
[40] D. Dudley, W. Duncan, J. Slaughter, Emerging digital micromirror device (dmd) applications, Proc. SPIE 4985 (2003) 1.
[41] J.R. Tumbleston, D. Shirvanyants, N. Ermoshkin, R. Janusziewicz, A.R. Johnson, D. Kelly, K. Chen, R. Pinschmidt, J.P. Rolland, A. Ermoshkin, et al., Continuous liquid interface production of 3d objects, Science 347 (6228) (2015) 1349–1352 (aaa2397).
[42] A. Ovsianikov, S. Schlie, A. Ngezahayo, A. Haverich, B.N. Chichkov, Two-photon polymerization technique for microfabrication of cad-designed 3d scaffolds from commercially available photosensitive materials, J. Tissue Eng. Regen. Med. 1 (6) (2007) 443–449.
[43] T. Weiß, G. Hildebrand, R. Schade, K. Liefeith, Two-photon polymerization for microfabrication of three-dimensional scaffolds for tissue engineering application, Engineering in Life Sciences 9 (5) (2009) 384–390.
[44] F. Claeyssens, E.A. Hasan, A. Gaidukeviciute, D.S. Achilleos, A. Ranella, C. Reinhardt, A. Ovsianikov, X. Shizhou, C. Fotakis, M. Vamvakaki, et al., Three-dimensional biodegradable structures fabricated by two-photon polymerization, Langmuir 25 (5) (2009) 3219–3223.
[45] A. Ovsianikov, A. Deiwick, S. Van Vlierberghe, P. Dubruel, L. Moller, G. Drager, B. Chichkov, Laser fabrication of three-dimensional cad scaffolds from photosensitive gelatin for applications in tissue engineering, Biomacromolecules 12 (4) (2011) 851–858.
[46] R. Felfel, L. Poocza, M. Gimeno-Fabra, T. Milde, G. Hildebrand, I. Ahmed, C. Scotchford, V. Sottile, D.M. Grant, K. Liefeith, In vitro degradation and mechanical properties of pla-pcl copolymer unit cell scaffolds generated by two-photon polymerization, Biomed. Mater. 11 (1) (2016) 015011.
[47] M.N. Cooke, J.P. Fisher, D. Dean, C. Rimnac, A.G. Mikos, Use of stereolithography to manufacture critical-sized 3d biodegradable scaffolds for bone ingrowth, J. Biomed. Mater. Res. B Appl. Biomater. 64 (2) (2003) 65–69.
[48] Y. Luo, C.K. Dolder, J.M. Walker, R. Mishra, D. Dean, M.L. Becker, Synthesis and biological evaluation of well-defined poly (propylene fumarate) oligomers and their use in 3d printed scaffolds, Biomacromolecules 17 (2) (2016) 690–697.
[49] T. Matsuda, M. Mizutani, Liquid acrylate-endcapped biodegradable poly (-caprolactone-co-trimethylene carbonate). II. Computer-aided stereolithographic microarchitectural surface photoconstructs, J. Biomed. Mater. Res. A 62 (3) (2002) 395–403.
[50] F.P. Melchels, J. Feijen, D.W. Grijpma, A poly (D, L-lactide) resin for the preparation of tissue engineering scaffolds by stereolithography, Biomaterials 30 (23) (2009) 3801–3809.
[51] J. Jansen, F.P. Melchels, D.W. Grijpma, J. Feijen, Fumaric acid monoethyl ester-functionalized poly (D, L-lactide)/n-vinyl-2-pyrrolidone resins for the preparation of tissue engineering scaffolds by stereolithography, Biomacromolecules 10 (2) (2008) 214–220.
[52] K. Arcaute, B. Mann, R. Wicker, Stereolithography of spatially controlled multi-material bioactive poly (ethylene glycol) scaffolds, Acta Biomater. 6 (3) (2010) 1047–1054.
[53] L. Elomaa, S. Teixeira, R. Hakala, H. Korhonen, D.W. Grijpma, J.V. Seppälä, Preparation of poly (ε-caprolactone)-based tissue engineering scaffolds by stereolithography, Acta Biomater. 7 (11) (2011) 3850–3856.
[54] Y.-L. Cheng, Y.-W. Chen, K. Wang, M.-Y. Shie, Enhanced adhesion and differentiation of human mesenchymal stem cell inside apatite-mineralized/poly (dopamine)-coated poly (ε-caprolactone) scaffolds by stereolithography, J. Mater. Chem. B 4 (38) (2016) 6307–6315.
[55] W. Zhou, D. Li, H. Wang, A novel aqueous ceramic suspension for ceramic stereolithography, Rapid Prototyp. J. 16 (1) (2010) 29–35.
[56] W. Bian, D. Li, Q. Lian, W. Zhang, L. Zhu, X. Li, Z. Jin, Design and fabrication of a novel porous implant with pre-set channels based on ceramic stereolithography for vascular implantation, Biofabrication 3 (3) (2011) 034103.
[57] O. Guillaume, M. Geven, D. Grijpma, T. Tang, L. Qin, Y. Lai, H. Yuan, R. Richards, D. Eglin, Poly (trimethylene carbonate) and nano-hydroxyapatite porous scaffolds manufactured by stereolithography, Polym. Adv. Technol. (2016) (Received: 30 June 2016, Accepted: 30 July 2016, Published online in Wiley Online Library).
[58] J. Wang, A. Goyanes, S. Gaisford, A.W. Basit, Stereolithographic (sla) 3d printing of oral modified-release dosage forms, Int. J. Pharm. 503 (1) (2016) 207–212.
[59] M.E. García-Sánchez, J.A. Perez-Naitoh, D.E. Ramirez-Arreola, J.R. Robledo-Ortíz, P. Ortega-Gudiño, I. Jiménez-Palomar, Characterization of ceramic-hydrogel composites for use in bone scaffolds made using additive manufacturing techniques, MRS Advances (2016) 1–6.
[60] S. Sánchez-Salcedo, A. Nieto, M. Vallet-Regí, Hydroxyapatite/β-tricalcium phosphate/agarose macroporous scaffolds for bone tissue engineering, Chem. Eng. J. 137 (1) (2008) 62–71.
[61] H. Wu, S. Lei, A review of bone graft substitutes made from ha-polymer composite scaffolds and fabrication potential with laser-based additive manufacturing processes, ASME 2015 International Manufacturing Science and Engineering Conference, American Society of Mechanical Engineers, 2015 (pp. V001T02A107–V001T02A107).
[62] S.F.S. Shirazi, S. Gharehkhani, M. Mehrali, H. Yarmand, H.S.C. Metselaar, N.A. Kadri, N.A.A. Osman, A review on powder-based additive manufacturing for tissue engineering: selective laser sintering and inkjet 3d printing, Sci. Technol. Adv. Mater. 16 (3) (2015) 033502.
[63] K.C. Kolan, M.C. Leu, G.E. Hilmas, M. Velez, Effect of material, process parameters, and simulated body fluids on mechanical properties of 13-93 bioactive glass porous constructs made by selective laser sintering, J. Mech. Behav. Biomed. Mater. 13 (2012) 14–24.
[64] G.V. Salmoria, P. Klauss, R.A. Paggi, L.A. Kanis, A. Lago, Structure and mechanical properties of cellulose based scaffolds fabricated by selective laser sintering, Polym. Test. 28 (6) (2009) 648–652.
[65] J.M. Williams, A. Adewunmi, R.M. Schek, C.L. Flanagan, P.H. Krebsbach, S.E. Feinberg, S.J. Hollister, S. Das, Bone tissue engineering using polycaprolactone scaffolds fabricated via selective laser sintering, Biomaterials 26 (23) (2005) 4817–4827.
[66] G. Ciardelli, V. Chiono, G. Vozzi, M. Pracella, A. Ahluwalia, N. Barbani, C. Cristallini, P. Giusti, Blends of poly-(ε-caprolactone) and polysaccharides in tissue engineering applications, Biomacromolecules 6 (4) (2005) 1961–1976.
[67] S. Eosoly, D. Brabazon, S. Lohfeld, L. Looney, Selective laser sintering of hydroxyapatite/poly-ε-caprolactone scaffolds, Acta Biomater. 6 (7) (2010) 2511–2517.
[68] B. Duan, W.L. Cheung, M. Wang, Optimized fabrication of ca–p/phbv nanocomposite scaffolds via selective laser sintering for bone tissue engineering, Biofabrication 3 (1) (2011) 015001.
[69] K.C. Kolan, M.C. Leu, G.E. Hilmas, R.F. Brown, M. Velez, Fabrication of 13-93 bioactive glass scaffolds for bone tissue engineering using indirect selective laser sintering, Biofabrication 3 (2) (2011) 025004.
[70] B. Duan, M. Wang, W.Y. Zhou, W.L. Cheung, Z.Y. Li, W.W. Lu, Three-dimensional nanocomposite scaffolds fabricated via selective laser sintering for bone tissue engineering, Acta Biomater. 6 (12) (2010) 4495–4505.
[71] M. Savalani, L. Hao, P. Dickens, Y. Zhang, K. Tanner, R. Harris, The effects and interactions of fabrication parameters on the properties of selective laser sintered hydroxyapatite polyamide composite biomaterials, Rapid Prototyp. J. 18 (1) (2012) 16–27.
[72] F. L. Amorim, A. Lohrengel, V. Neubert, C. F. Higa, T. Czelusniak, Selective laser sintering of mo-cuni composite to be used as edm electrode, Rapid Prototyp. J. 20 (1) (2014) 59–68.
[73] K. Tan, C. Chua, K. Leong, C. Cheah, P. Cheang, M.A. Bakar, S. Cha, Scaffold development using selective laser sintering of polyetheretherketone–hydroxyapatite biocomposite blends, Biomaterials 24 (18) (2003) 3115–3123.
[74] C. Shuai, C. Gao, Y. Nie, H. Hu, Y. Zhou, S. Peng, Structure and properties of nano-hydroxypatite scaffolds for bone tissue engineering with aselective laser sintering system, Nanotechnology 22 (28) (2011) 285703.
[75] W.Y. Zhou, M. Wang, W.L. Cheung, W.Y. Ip, Selective laser sintering of poly (L-lactide)/carbonated hydroxyapatite nanocomposite porous scaffolds for bone tissue engineering, Tissue Eng. (2010) 179–204.
[76] B. Duan, M. Wang, Customized ca–p/phbv nanocomposite scaffolds for bone tissue engineering: design, fabrication, surface modification and sustained release of growth factor, J. R. Soc. Interface 7 (2010) S615–S629.
[77] B. Duan, M. Wang, Encapsulation and release of biomolecules from ca–p/phbv nanocomposite microspheres and three-dimensional scaffolds fabricated by selective laser sintering, Polym. Degrad. Stab. 95 (9) (2010) 1655–1664.
[78] B. Duan, M. Wang, Customized nanocomposite scaffolds fabricated via selective laser sintering for bone tissue engineering, Handbook of Intelligent Scaffold for Tissue Engineering and Regenerative Medicine, Pan Stanford Publishing, 2012, pp. 925–953.
[79] B. Duan, M. Wang, Z.Y. Li, W.C. Chan, W.W. Lu, Surface modification of three-dimensional ca-p/phbv nanocomposite scaffolds by physical entrapment of gelatin and its in vitro biological evaluation, Front. Mater. Sci. 5 (1) (2011) 57–68.
[80] H.-T. Liao, M.-Y. Lee, W.-W. Tsai, H.-C. Wang, W.-C. Lu, Osteogenesis of adipose-derived stem cells on polycaprolactone–β-tricalcium phosphate scaffold fabricated via selective laser sintering and surface coating with collagen type I, J. Tissue Eng. Regen. Med. 10 (10) (2010) (Published online in Wiley Online Library).
[81] H. Doyle, S. Lohfeld, P. McHugh, Evaluating the effect of increasing ceramic content on the mechanical properties, material microstructure and degradation of selective laser sintered polycaprolactone/β-tricalcium phosphate materials, Med. Eng. Phys. 37 (8) (2015) 767–776.
[82] P. Feng, M. Niu, C. Gao, S. Peng, C. Shuai, A novel two-step sintering for nano-hydroxyapatite scaffolds for bone tissue engineering, Sci. Rep. 4 (2014) 5599.

[83] A. Mazzoli, C. Ferretti, A. Gigante, E. Salvolini, M. Mattioli-Belmonte, Selective laser sintering manufacturing of polycaprolactone bone scaffolds for applications in bone tissue engineering, Rapid Prototyp. J. 21 (4) (2015) 386–392.
[84] S. Lee, W.Y. Zhou, M. Wang, W. Cheung, W. Ip, Selective laser sintering of poly (L-lactide) porous scaffolds for bone tissue engineering, Journal of Biomimetics, Biomaterials and Tissue Engineering, vol. 1, Trans Tech Publ, 2009, pp. 81–89.
[85] T. Pereira, M. Silva, M. Oliveira, I. Maia, J. Silva, M. Costa, R. Thiré, Effect of process parameters on the properties of selective laser sintered poly (3-hydroxybutyrate) scaffolds for bone tissue engineering, Virtual and Physical Prototyping 7 (4) (2012) 275–285.
[86] F. Wiria, K. Leong, C. Chua, Y. Liu, Poly-ε-caprolactone/hydroxyapatite for tissue engineering scaffold fabrication via selective laser sintering, Acta Biomater. 3 (1) (2007) 1–12.
[87] S. Eshraghi, S. Das, Micromechanical finite-element modeling and experimental characterization of the compressive mechanical properties of polycaprolactone–hydroxyapatite composite scaffolds prepared by selective laser sintering for bone tissue engineering, Acta Biomater. 8 (8) (2012) 3138–3143.
[88] K. Tan, C. Chua, K. Leong, M. Naing, C. Cheah, Fabrication and characterization of three-dimensional poly (ether-ether-ketone)/-hydroxyapatite biocomposite scaffolds using laser sintering, Proc. Inst. Mech. Eng. H J. Eng. Med. 219 (3) (2005) 183–194.
[89] K. Kesenci, L. Fambri, C. Migliaresi, E. Piskin, Preparation and properties of poly (L-lactide)/hydroxyapatite composites, J. Biomater. Sci. Polym. Ed. 11 (6) (2000) 617–632.
[90] C. Shuai, P. Wu, Y. Zhong, P. Feng, C. Gao, W. Huang, Z. Zhou, L. Chen, C. Shuai, Polyetheretherketone/poly (glycolic acid) blend scaffolds with biodegradable properties, J. Biomater. Sci. Polym. Ed. 27 (14) (2016) 1434–1446.
[91] D. Kuznetsova, P. Timashev, V. Dudenkova, A. Meleshina, E. Antonov, L. Krotova, V. Popov, V. Bagratashvili, E. Zagaynova, Comparative analysis of proliferation and viability of multipotent mesenchymal stromal cells in 3d scaffolds with different architectonics, Bull. Exp. Biol. Med. 160 (4) (2016) 535–541.
[92] C. Shuai, Z. Mao, H. Lu, Y. Nie, H. Hu, S. Peng, Fabrication of porous polyvinyl alcohol scaffold for bone tissue engineering via selective laser sintering, Biofabrication 5 (1) (2013) 015014.
[93] S. XiaoHui, L. Wei, S. PingHui, S. QingYong, W. QingSong, S. YuSheng, L. Kai, L. WenGuang, Selective laser sintering of aliphatic-polycarbonate/hydroxyapatite composite scaffolds for medical applications, Int. J. Adv. Manuf. Technol. 81 (1–4) (2015) 15–25.
[94] C. Shuai, J. Zhuang, S. Peng, X. Wen, Inhibition of phase transformation from β-to α-tricalcium phosphate with addition of poly (L-lactic acid) in selective laser sintering, Rapid Prototyp. J. 20 (5) (2014) 369–376.
[95] A. Houben, J. Van Hoorick, J. Van Erps, H. Thienpont, S. Van Vlierberghe, P. Dubruel, Indirect rapid prototyping: opening up unprecedented opportunities in scaffold design and applications, Ann. Biomed. Eng. 45 (1) (2017) 58–83.
[96] F. Probst, D. Hutmacher, D. Müller, H. Machens, J. Schantz, Calvarial reconstruction by customized bioactive implant, Handchirurgie, Mikrochirurgie, plastische Chirurgie: Organ der Deutschsprachigen Arbeitsgemeinschaft fur Handchirurgie: Organ der Deutschsprachigen Arbeitsgemeinschaft fur Mikrochirurgie der Peripheren Nerven und Gefasse, Organ der V. 42 (6) (2010) 369–373.
[97] C.-P. Jiang, Y.-Y. Chen, Biofabrication of hybrid bone scaffolds using a dual-nozzle bioplotter and in-vitro study of osteoblast cell, Int. J. Precis. Eng. Manuf. 15 (9) (2014) 1947–1953.
[98] F. Pati, T.-H. Song, G. Rijal, J. Jang, S.W. Kim, D.-W. Cho, Ornamenting 3d printed scaffolds with cell-laid extracellular matrix for bone tissue regeneration, Biomaterials 37 (2015) 230–241.
[99] D.W. Hutmacher, T. Schantz, I. Zein, K.W. Ng, S.H. Teoh, K.C. Tan, Mechanical properties and cell cultural response of polycaprolactone scaffolds designed and fabricated via fused deposition modeling, J. Biomed. Mater. Res. A 55 (2) (2001) 203–216.
[100] D. Rohner, D.W. Hutmacher, T.K. Cheng, M. Oberholzer, B. Hammer, In vivo efficacy of bone-marrow-coated polycaprolactone scaffolds for the reconstruction of orbital defects in the pig, J. Biomed. Mater. Res. B Appl. Biomater. 66 (2) (2003) 574–580.
[101] J.C. Reichert, S. Saifzadeh, M.E. Wullschleger, D.R. Epari, M.A. Schütz, G.N. Duda, H. Schell, M. van Griensven, H. Redl, D.W. Hutmacher, The challenge of establishing preclinical models for segmental bone defect research, Biomaterials 30 (12) (2009) 2149–2163.
[102] J.-T. Schantz, T.-C. Lim, C. Ning, S.H. Teoh, K.C. Tan, S.C. Wang, D.W. Hutmacher, Cranioplasty after trephination using a novel biodegradable burr hole cover: technical case report, Operative Neurosurgery 58 (1) (2006) (ONS–E176).
[103] H.-W. Kang, S.J. Lee, I.K. Ko, C. Kengla, J.J. Yoo, A. Atala, A 3d bioprinting system to produce human-scale tissue constructs with structural integrity, Nat. Biotechnol. 34 (3) (2016) 312.
[104] A. Bégin-Drolet, M.-A. Dussault, S.A. Fernandez, J. Larose-Dutil, R.L. Leask, C.A. Hoesli, J. Ruel, Design of a 3d printer head for additive manufacturing of sugar glass for tissue engineering applications, Additive Manufacturing 15 (2017) 29–39.
[105] K. Schütz, A.-M. Placht, B. Paul, S. Brüggemeier, M. Gelinsky, A. Lode, Three-dimensional plotting of a cell-laden alginate/methylcellulose blend: towards biofabrication of tissue engineering constructs with clinically relevant dimensions, J. Tissue Eng. Regen. Med. 11 (2017) 1574–1587.
[106] S. Giron, A. Lode, M. Gelinsky, In situ functionalization of scaffolds during extrusion-based 3d plotting using a piezoelectric nanoliter pipette, Journal of 3D Printing in Medicine 1 (1) (2017) 25–29.
[107] B. Holmes, K. Bulusu, M. Plesniak, L.G. Zhang, A synergistic approach to the design, fabrication and evaluation of 3d printed micro and nano featured scaffolds for vascularized bone tissue repair, Nanotechnology 27 (6) (2016) 064001.
[108] C.-T. Kao, C.-C. Lin, Y.-W. Chen, C.-H. Yeh, H.-Y. Fang, M.-Y. Shie, Poly (dopamine) coating of 3d printed poly (lactic acid) scaffolds for bone tissue engineering, Mater. Sci. Eng. C 56 (2015) 165–173.
[109] C.X. Lam, M.M. Savalani, S.-H. Teoh, D.W. Hutmacher, Dynamics of in vitro polymer degradation of polycaprolactone-based scaffolds: accelerated versus simulated physiological conditions, Biomed. Mater. 3 (3) (2008) 034108.
[110] S.J. Kalita, S. Bose, H.L. Hosick, A. Bandyopadhyay, Development of controlled porosity polymer-ceramic composite scaffolds via fused deposition modeling, Mater. Sci. Eng. C 23 (5) (2003) 611–620.
[111] H. Seyednejad, D. Gawlitta, W.J. Dhert, C.F. Van Nostrum, T. Vermonden, W.E. Hennink, Preparation and characterization of a three-dimensional printed scaffold based on a functionalized polyester for bone tissue engineering applications, Acta Biomater. 7 (5) (2011) 1999–2006.
[112] H. Seyednejad, D. Gawlitta, R.V. Kuiper, A. de Bruin, C.F. van Nostrum, T. Vermonden, W.J. Dhert, W.E. Hennink, In vivo biocompatibility and biodegradation of 3d-printed porous scaffolds based on a hydroxyl-functionalized poly (ε-caprolactone), Biomaterials 33 (17) (2012) 4309–4318.
[113] T. Ahlfeld, A.R. Akkineni, Y. Förster, T. Köhler, S. Knaack, M. Gelinsky, A. Lode, Design and fabrication of complex scaffolds for bone defect healing: combined 3d plotting of a calcium phosphate cement and a growth factor-loaded hydrogel, Ann. Biomed. Eng. 45 (1) (2017) 224–236.
[114] W. Schuurman, V. Khristov, M.W. Pot, P.R. van Weeren, W.J. Dhert, J. Malda, Bioprinting of hybrid tissue constructs with tailorable mechanical properties, Biofabrication 3 (2) (2011) 021001.
[115] W. Schuurman, P.A. Levett, M.W. Pot, P.R. van Weeren, W.J. Dhert, D.W. Hutmacher, F.P. Melchels, T.J. Klein, J. Malda, Gelatin-methacrylamide hydrogels as potential biomaterials for fabrication of tissue-engineered cartilage constructs, Macromol. Biosci. 13 (5) (2013) 551–561.
[116] R. Detsch, F. Uhl, U. Deisinger, G. Ziegler, 3d-cultivation of bone marrow stromal cells on hydroxyapatite scaffolds fabricated by dispense-plotting and negative mould technique, J. Mater. Sci. Mater. Med. 19 (4) (2008) 1491–1496.
[117] A. Lode, K. Meissner, Y. Luo, F. Sonntag, S. Glorius, B. Nies, C. Vater, F. Despang, T. Hanke, M. Gelinsky, Fabrication of porous scaffolds by three-dimensional plotting of a pasty calcium phosphate bone cement under mild conditions, J. Tissue Eng. Regen. Med. 8 (9) (2014) 682–693.
[118] Q. Fu, E. Saiz, A.P. Tomsia, Bioinspired strong and highly porous glass scaffolds, Adv. Funct. Mater. 21 (6) (2011) 1058–1063.
[119] C. Wu, Y. Luo, G. Cuniberti, Y. Xiao, M. Gelinsky, Three-dimensional printing of hierarchical and tough mesoporous bioactive glass scaffolds with a controllable pore architecture, excellent mechanical strength and mineralization ability, Acta Biomater. 7 (6) (2011) 2644–2650.
[120] A. Martins, S. Chung, A.J. Pedro, R.A. Sousa, A.P. Marques, R.L. Reis, N.M. Neves, Hierarchical starch-based fibrous scaffold for bone tissue engineering applications, J. Tissue Eng. Regen. Med. 3 (1) (2009) 37–42.
[121] C.R. Almeida, T. Serra, M.I. Oliveira, J.A. Planell, M.A. Barbosa, M. Navarro, Impact of 3-d printed pla-and chitosan-based scaffolds on human monocyte/macrophage responses: unraveling the effect of 3-d structures on inflammation, Acta Biomater. 10 (2) (2014) 613–622.
[122] N.E. Fedorovich, J.R. De Wijn, A.J. Verbout, J. Alblas, W.J. Dhert, Three-dimensional fiber deposition of cell-laden, viable, patterned constructs for bone tissue printing, Tissue Eng. A 14 (1) (2008) 127–133.
[123] J. P. Vacanti, L. G. Cima, M. J. Cima, Vascularized tissue regeneration matrices formed by solid free form fabrication techniques, US Patent 6,139,574 (Oct. 31 2000).
[124] A. Butscher, M. Bohner, C. Roth, A. Ernstberger, R. Heuberger, N. Doebelin, P.R. Von Rohr, R. Müller, Printability of calcium phosphate powders for three-dimensional printing of tissue engineering scaffolds, Acta Biomater. 8 (1) (2012) 373–385.
[125] A. Curodeau, E. Sachs, S. Caldarise, Design and fabrication of cast orthopedic implants with freeform surface textures from 3-d printed ceramic shell, J. Biomed. Mater. Res. A 53 (5) (2000) 525–535.
[126] Z. Zhou, F. Buchanan, C. Mitchell, N. Dunne, Printability of calcium phosphate: calcium sulfate powders for the application of tissue engineered bone scaffolds using the 3d printing technique, Mater. Sci. Eng. C 38 (2014) 1–10.
[127] H. Seitz, U. Deisinger, B. Leukers, R. Detsch, G. Ziegler, Different calcium phosphate granules for 3-d printing of bone tissue engineering scaffolds, Adv. Eng. Mater. 11 (2009) B41–B46.
[128] S. Tarafder, V.K. Balla, N.M. Davies, A. Bandyopadhyay, S. Bose, Microwave-sintered 3d printed tricalcium phosphate scaffolds for bone tissue engineering, J. Tissue Eng. Regen. Med. 7 (8) (2013) 631–641.
[129] S. Amirkhani, R. Bagheri, A.Z. Yazdi, Effect of pore geometry and loading direction on deformation mechanism of rapid prototyped scaffolds, Acta Mater. 60 (6) (2012) 2778–2789.
[130] B. Leukers, H. Gülkan, S.H. Irsen, S. Milz, C. Tille, M. Schieker, H. Seitz, Hydroxyapatite scaffolds for bone tissue engineering made by 3d printing, J. Mater. Sci. Mater. Med. 16 (12) (2005) 1121–1124.
[131] R. Meszaros, R. Zhao, N. Travitzky, T. Fey, P. Greil, L. Wondraczek, Three-dimensional printing of a bioactive glass, Glass Technology-European Journal of Glass Science and Technology Part A 52 (4) (2011) 111–116.
[132] C.X.F. Lam, X. Mo, S.-H. Teoh, D. Hutmacher, Scaffold development using 3d printing with a starch-based polymer, Mater. Sci. Eng. C 20 (1) (2002) 49–56.
[133] J. Will, R. Melcher, C. Treul, N. Travitzky, U. Kneser, E. Polykandriotis, R. Horch, P. Greil, Porous ceramic bone scaffolds for vascularized bone tissue regeneration, J. Mater. Sci. Mater. Med. 19 (8) (2008) 2781–2790.

[134] G.A. Fielding, A. Bandyopadhyay, S. Bose, Effects of silica and zinc oxide doping on mechanical and biological properties of 3d printed tricalcium phosphate tissue engineering scaffolds, Dent. Mater. 28 (2) (2012) 113–122.
[135] S.T. Becker, H. Bolte, O. Krapf, H. Seitz, T. Douglas, S. Sivananthan, J. Wiltfang, E. Sherry, P.H. Warnke, Endocultivation: 3d printed customized porous scaffolds for heterotopic bone induction, Oral Oncol. 45 (11) (2009) e181–e188.
[136] R. Detsch, S. Schaefer, U. Deisinger, G. Ziegler, H. Seitz, B. Leukers, In vitro-osteoclastic activity studies on surfaces of 3d printed calcium phosphate scaffolds, J. Biomater. Appl. 26 (2011) 359–380 (September).
[137] F.C. Fierz, F. Beckmann, M. Huser, S.H. Irsen, B. Leukers, F. Witte, Ö. Degistirici, A. Andronache, M. Thie, B. Müller, The morphology of anisotropic 3d-printed hydroxyapatite scaffolds, Biomaterials 29 (28) (2008) 3799–3806.
[138] U. Gbureck, T. Hölzel, C.J. Doillon, F.A. Mueller, J.E. Barralet, Direct printing of bioceramic implants with spatially localized angiogenic factors, Adv. Mater. 19 (6) (2007) 795–800.
[139] P. Habibovic, U. Gbureck, C.J. Doillon, D.C. Bassett, C.A. van Blitterswijk, J.E. Barralet, Osteoconduction and osteoinduction of low-temperature 3d printed bioceramic implants, Biomaterials 29 (7) (2008) 944–953.
[140] Z. Ge, X. Tian, B.C. Heng, V. Fan, J.F. Yeo, T. Cao, Histological evaluation of osteogenesis of 3d-printed poly-lactic-co-glycolic acid (plga) scaffolds in a rabbit model, Biomed. Mater. 4 (2) (2009) 021001.
[141] J.A. Inzana, D. Olvera, S.M. Fuller, J.P. Kelly, O.A. Graeve, E.M. Schwarz, S.L. Kates, H.A. Awad, 3d printing of composite calcium phosphate and collagen scaffolds for bone regeneration, Biomaterials 35 (13) (2014) 4026–4034.
[142] S.N. Rath, L.A. Strobel, A. Arkudas, J.P. Beier, A.-K. Maier, P. Greil, R.E. Horch, U. Kneser, Osteoinduction and survival of osteoblasts and bone-marrow stromal cells in 3d biphasic calcium phosphate scaffolds under static and dynamic culture conditions, J. Cell. Mol. Med. 16 (10) (2012) 2350–2361.
[143] R. Chumnanklang, T. Panyathanmaporn, K. Sitthiseripratip, J. Suwanprateeb, 3d printing of hydroxyapatite: effect of binder concentration in pre-coated particle on part strength, Mater. Sci. Eng. C 27 (4) (2007) 914–921.
[144] A. Khalyfa, S. Vogt, J. Weisser, G. Grimm, A. Rechtenbach, W. Meyer, M. Schnabelrauch, Development of a new calcium phosphate powder-binder system for the 3d printing of patient specific implants, J. Mater. Sci. Mater. Med. 18 (5) (2007) 909–916.
[145] U. Gbureck, T. Hölzel, I. Biermann, J.E. Barralet, L.M. Grover, Preparation of tricalcium phosphate/calcium pyrophosphate structures via rapid prototyping, J. Mater. Sci. Mater. Med. 19 (4) (2008) 1559–1563.
[146] J. Suwanprateeb, R. Sanngam, W. Suvannapruk, T. Panyathanmaporn, Mechanical and in vitro performance of apatite–wollastonite glass ceramic reinforced hydroxyapatite composite fabricated by 3d-printing, J. Mater. Sci. Mater. Med. 20 (6) (2009) 1281.
[147] Y. Shanjani, D. Croos, J. Amritha, R.M. Pilliar, R.A. Kandel, E. Toyserkani, Solid freeform fabrication and characterization of porous calcium polyphosphate structures for tissue engineering purposes, J. Biomed. Mater. Res. B Appl. Biomater. 93 (2) (2010) 510–519.
[148] M. Castilho, C. Moseke, A. Ewald, U. Gbureck, J. Groll, I. Pires, J. Teßmar, E. Vorndran, Direct 3d powder printing of biphasic calcium phosphate scaffolds for substitution of complex bone defects, Biofabrication 6 (1) (2014) 015006.
[149] U. Gbureck, T. Hölzel, U. Klammert, K. Würzler, F.A. Müller, J.E. Barralet, Resorbable dicalcium phosphate bone substitutes prepared by 3d powder printing, Adv. Funct. Mater. 17 (18) (2007) 3940–3945.
[150] U. Gbureck, E. Vorndran, F.A. Müller, J.E. Barralet, Low temperature direct 3d printed bioceramics and biocomposites as drug release matrices, J. Control. Release 122 (2) (2007) 173–180.
[151] J.-Y. Lee, B. Choi, B. Wu, M. Lee, Customized biomimetic scaffolds created by indirect three-dimensional printing for tissue engineering, Biofabrication 5 (4) (2013) 045003.
[152] E. Tamjid, A. Simchi, J.W. Dunlop, P. Fratzl, R. Bagheri, M. Vossoughi, Tissue growth into three-dimensional composite scaffolds with controlled micro-features and nanotopographical surfaces, J. Biomed. Mater. Res. A 101 (10) (2013) 2796–2807.
[153] H. Ragelle, M.W. Tibbitt, S.-Y. Wu, M.A. Castillo, G.Z. Cheng, S.P. Gangadharan, D.G. Anderson, M.J. Cima, R. Langer, Surface tension-assisted additive manufacturing, Nat. Commun. 9 (1) (2018) 1184.
[154] F. Chapelin, A. Khurana, M. Moneeb, F.K.G. Hazard, C.F.R. Chan, H. Nejadnik, D. Gratzinger, S. Messing, J. Erdmann, A. Gaur, et al., Tumor formation of adult stem cell transplants in rodent arthritic joints, Mol. Imaging Biol. (2018) 1–10.